Cell Reports
Report

Cell PRESS
Open ACCESS

Local Functional Overconnectivity in Posterior Brain Regions Is Associated with Symptom Severity in Autism Spectrum Disorders

Christopher Lee Keown,[1,2] Patricia Shih,[3] Aarti Nair,[1,4] Nick Peterson,[1,5] Mark Edward Mulvey,[1,2] and Ralph-Axel Müller[1,4,*]
[1]Brain Development Imaging Laboratory, Department of Psychology, San Diego State University, San Diego, CA 92120, USA
[2]Computational Science Research Center, San Diego State University, San Diego, CA 92182, USA
[3]Neuroscience Department, Brown University, Providence, RI 02912, USA
[4]Joint Doctoral Program in Clinical Psychology, San Diego State University and University of California, San Diego, San Diego, CA 92182, USA
[5]Department of Mathematics and Statistics, San Diego State University, San Diego, CA 92182, USA
*Correspondence: rmueller@mail.sdsu.edu
http://dx.doi.org/10.1016/j.celrep.2013.10.003

SUMMARY

Although growing evidence indicates atypical long-distance connectivity in autism spectrum disorder (ASD), much less is known about local connectivity, despite conjectures that local overconnectivity may be causally involved in the disorder. Using functional connectivity MRI and graph theory, we found that local functional connectivity was atypically increased in adolescents with ASD in temporo-occipital regions bilaterally. Posterior overconnectivity was found to be associated with higher ASD symptom severity, whereas an ASD subsample with low severity showed frontal underconnectivity. The findings suggest links between symptomatology and local connectivity, which vary within the autism spectrum.

INTRODUCTION

Autism spectrum disorder (ASD) is a neurodevelopmental disorder of increasing prevalence, with recent estimates at 1%–2.5% (CDC, 2012; Kim et al., 2011). In the past decade, consensus has grown that sociocommunicative and other impairments in ASD relate to disturbances at the level of brain networks and connectivity (Geschwind and Levitt, 2007), as supported by findings of white matter growth anomalies in infants and toddlers (Courchesne et al., 2011a; Wolff et al., 2012) and white-matter compromise in children and adolescents (Shukla et al., 2011). In contrast to ample evidence from fMRI studies suggesting atypical (predominantly reduced) long-distance functional connectivity (Vissers et al., 2012), there is little firm knowledge about *local* connectivity in ASD. This is surprising given the evidence of abnormal cellular organization in cerebral cortex in ASD from postmortem studies (Amaral et al., 2008), in particular, findings suggesting atypically tight packing of cortical minicolumns with reduced lateral inhibition (Casanova and Trippe, 2009). Conjectures that local connectivity may be atypically enhanced (Belmonte et al., 2004a) have been largely based on indirect evidence, such as findings indicating increased cortical excitation/inhibition ratios (Rubenstein and Merzenich, 2003). Whereas resting-state functional connectivity MRI (rs-fcMRI) has become a method of choice for the study of long-distance connectivity (Van Dijk et al., 2010), its usefulness in assessing local connectivity has also been demonstrated in healthy adults (Sepulcre et al., 2010). We used rs-fcMRI implementing connection density measures from graph theory to examine local functional connectivity in adolescents with ASD and typically developing (TD) adolescents.

RESULTS

Both groups (Table 1), which were matched for head motion (see Experimental Procedures), showed relatively strong local connectivity in posterior cingulate cortex and precuneus, medial prefrontal cortex, and medial occipital lobe (including primary visual cortex; orange and red areas in Figures 1A and 1B), whereas the temporal lobes (except for posterior portions) showed relatively low connectivity (green and cyan areas in Figures 1A and 1B). Direct group comparisons yielded increased local connectivity in the ASD group in temporo-occipital regions (including inferior and middle temporal gyri, temporal pole, middle and superior occipital gyri, calcarine cortex, right parahippocampal gyrus, right fusiform gyrus, and left cuneus) and right middle and superior frontal gyri. Reduced local connectivity in the ASD group was detected only in small clusters in middle cingulate and right inferior parietal sites (Figure 1C; Table S1). Within the entire cerebral cortex, local connectivity density was positively correlated with Autism Diagnostic Observation Schedule (ADOS) (Lord et al., 2001) social reciprocity ($r = 0.40$; $p = 0.018$) and repetitive behavior scores ($r = 0.61$; $p < 0.001$), whereas no diagnostic correlations were found for local density in the cingulate and parietal underconnectivity clusters.

Given the observed diagnostic correlations, we examined regional patterns of local connectivity abnormalities in greater

Table 1. Participant Information

	TD Group	ASD Group	
n	29 (seven female)	29 (four female)	p
Handedness	25 R, 4 L	26 R, 3 L	
Age (years)	13.5 (2.2)	13.8 (2.4)	0.74
Verbal IQ	106.2 (9.5)	105.4 (20.9)	0.84
Nonverbal IQ	108.1 (10.0)	106.3 (18.5)	0.65
Full-scale IQ	108.0 (8.9)	107.9 (19.0)	0.97
Head motion (rmsd)	0.15 (.14)	0.14 (.11)	0.78
ADOS Algorithm Scores			
Social reciprocity	-	8.2	-
Communication	-	3.4	-
Repetitive behavior	-	2.1	-

rmsd, root-mean-square displacement; R, right; L, left; IQ and ADOS scores missing for one ASD participant.

depth by dividing our ASD cohort into high and low symptom severity subgroups. We applied an algorithm, using predefined quantitative criteria (see Experimental Procedures) to optimally partition the ASD sample into two subgroups (Table S2) that differed maximally on ADOS social and repetitive behavior scores while being maximally matched for head motion, which is crucial for local connectivity analyses (Power et al., 2012; Satterthwaite et al., 2013; Tyszka et al., 2013; Van Dijk et al., 2012). For the higher-severity subgroup, we found extensive clusters of exclusive overconnectivity, predominantly in posterior brain regions (Figure 1D; Table S3). The low-severity subgroup showed a very different pattern, characterized by widespread local *underconnectivity* in left lateral and bilateral polar and medial frontal cortices, with limited overconnectivity in temporo-occipital regions (Figure 1E; Table S4). For all regions showing local connectivity abnormalities in either high- or low-severity groups combined (all clusters in Figures 1D and 1E), we found significant correlations between local connectivity and ADOS social scores ($r = 0.41$; $p = 0.015$) and repetitive behavior scores ($r = 0.68$; $p < 0.001$; Figure 2).

DISCUSSION

Whereas both TD and ASD groups showed overall patterns of local connectivity consistent with previous results for healthy adults (Sepulcre et al., 2010), significant group differences were detected, which overwhelmingly reflected increases of local connectivity in the ASD group, with clusters in primary visual and extrastriate cortices, extending into the temporal lobe (Figure 1C). Except for small clusters in the right frontal lobe, no local overconnectivity was detected in anterior brain regions. Conversely, local underconnectivity was observed in ASD participants with low symptom severity occurring exclusively in anterior brain regions across the frontal lobe.

Widespread local overconnectivity in our cohort of adolescents with ASD partially supports an earlier hypothesis (Belmonte et al., 2004b; Rippon et al., 2007), for which little direct empirical evidence has been available thus far (see review in Vissers et al. [2012]). However, overconnectivity was almost exclusively detected in adolescents with higher symptom severity and occurred predominantly in posterior brain regions, i.e., in regions that participate in visual processing. This regional pattern of overconnectivity is remarkable in view of existing evidence suggesting that vision may have a special status in the neuropsychological profile of ASD, including islands of superior function (Simmons et al., 2009). Specifically, many visual studies have indicated a preference for local processing in ASD, potentially at the expense of global gestalt processing (Dakin and Frith, 2005), which is consistent with the more general model of "weak central coherence" (Happé, 1999). Local processing strengths are supported by more robust evidence than global processing weaknesses (Dakin and Frith, 2005), which may suggest that visual perception is actually generally enhanced in ASD (Mottron et al., 2006). This appears consistent with atypical participation of visual cortices across various tasks, including nonvisual ones (Samson et al., 2012; Shen et al., 2012), in ASD.

Only two small clusters of reduced local connectivity were detected in the full ASD sample, compared to the TD group, occurring in middle cingulate and right inferior parietal cortex. However, such effects were more pronounced in the low-severity ASD subsample, with numerous clusters in the frontal lobe, which included bilateral medial portions close to the frontal pole, as well as more posterior lateral frontal cortices in the left hemisphere (Figure 1E). Whereas it is tempting to relate our findings to impaired executive function and cognitive control in ASD (Hill, 2004), such impairment would be predominantly expected in lower-functioning children with ASD. The functional and developmental significance of our findings may therefore lie in what appears to be an atypical gradient of local connectivity abnormalities from mild anterior underconnectivity to robust posterior overconnectivity in ASD. In higher-severity ASD, the distribution of this gradient was found shifted toward overconnectivity. Anterior-posterior gradients have been observed with respect to the expression of ASD-related genes (State and Šestan, 2012) and early gray matter overgrowth (Courchesne et al., 2011b), possibly linked to the gradients for local connectivity detected here. However, it remains to be determined whether frontal underconnectivity seen in low-severity participants may reflect a compensatory response to early frontal gray matter overgrowth and neuronal overproliferation.

When considering biological mechanisms that may underlie observed atypical connectivity, caution is advised because the concept of "local connectivity" remains loosely defined. Blood-oxygen-level-dependent (BOLD) correlations across neighboring voxels may be driven by large numbers of local neuronal assemblies with predominantly excitatory interconnectivity. Local overconnectivity in posterior cortices could thus be considered compatible with postmortem findings of reduced lateral inhibition between densely packed minicolumns in ASD (Casanova and Trippe, 2009). However, differences in spatial scale (with minicolumns measuring c. 30–80 μm contrasted by a 14 mm radius for connectivity density implemented here) preclude any firm mechanistic interpretations.

In summary, our findings show widespread local overconnectivity in ASD but require two crucial qualifications: (1) We observed an anterior-posterior gradient of local connectivity, with predominant overconnectivity in posterior regions

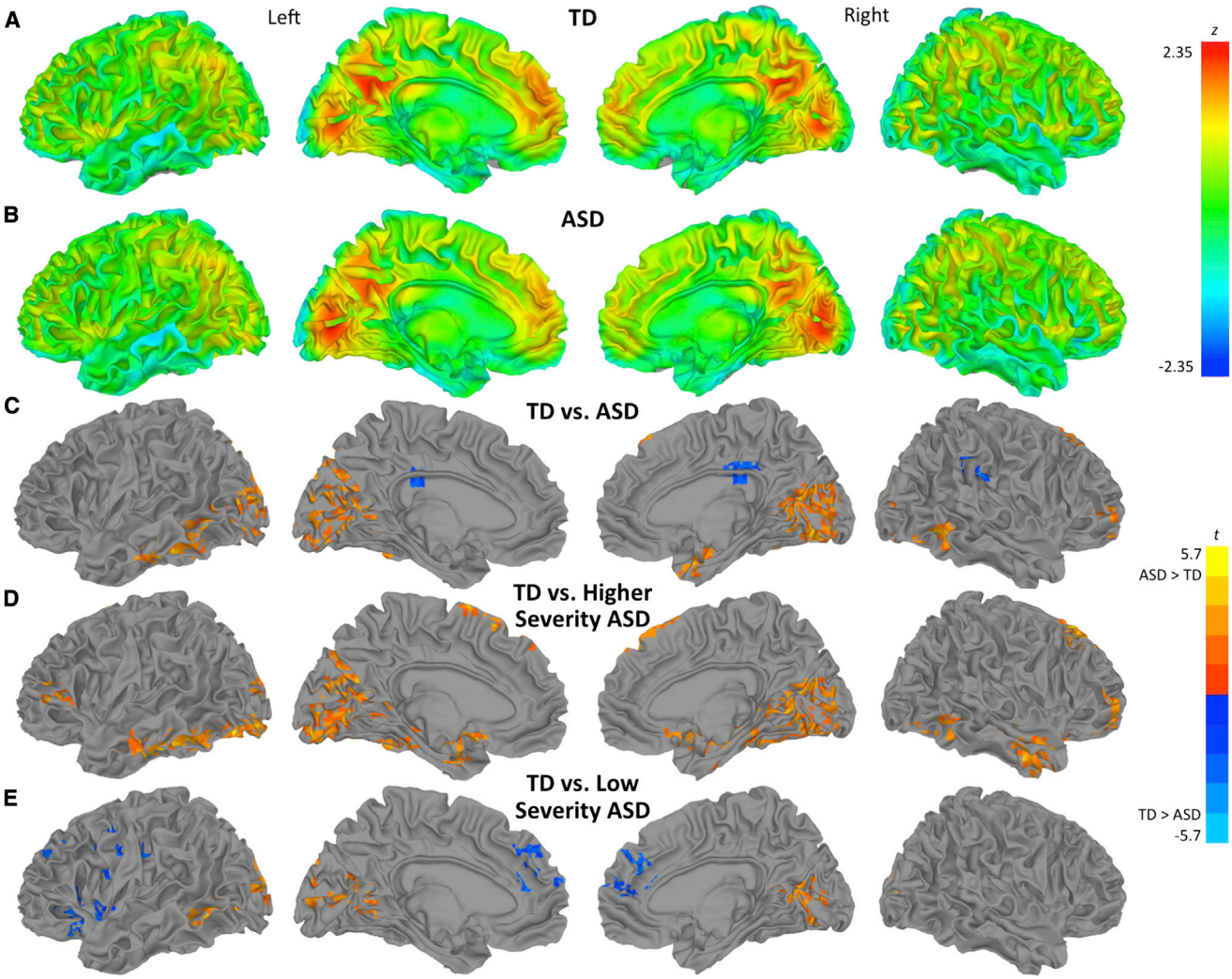

Figure 1. Within- and Between-Group Maps for Local Connection Density

(A–E) Surface renderings of local connectivity density for TD (A) and ASD groups (B). Greater *Z* scores correspond to brain regions with high connectivity (red scale). Clusters of significant group differences in local degrees ($p < 0.05$; corrected [corr.]) for entire ASD cohort (C) as well as for higher-severity (D) and low-severity (E) ASD subgroups in comparison to the TD group (warm colors: ASD > TD; cool colors TD > ASD).

accompanied by some regions of underconnectivity in frontal cortices seen in children with low-severity ASD. (2) Overconnectivity was linked to symptom severity, i.e., it was found predominantly in adolescents with higher-severity ASD, whereas those with low severity showed a mixed pattern of local connectivity being decreased in anterior and increased in posterior brain regions.

EXPERIMENTAL PROCEDURES

Participants

MRI data were collected from 37 high-functioning adolescents with ASD and 33 typically developing control participants. Six ASD participants with excessive head motion (see below) were excluded from the analysis. Two further ASD and four TD participants were excluded to restore group matching on age, handedness, and nonverbal IQ, resulting in a final sample of 29 ASD and 29 TD participants (Table 1). IQ was quantified using the Wechsler Abbreviated Scale of Intelligence (Wechsler, 1999), and handedness was determined by the Edinburgh Handedness Inventory (Oldfield, 1971). Clinical diagnoses were confirmed using the Autism Diagnostic Interview-Revised (Rutter et al., 2003), ADOS (Lord et al., 2001), and expert clinical judgment according to DSM-IV-TR criteria (American Psychiatric Association, 2000). Children with ASD-related medical conditions (e.g., fragile-X syndrome and tuberous sclerosis) or other neurological conditions (e.g., epilepsy and Tourette's syndrome) were excluded. Participants in the TD group had no reported history of ASD as well as no reported history of any other neurological or psychiatric conditions. All participants and caregivers gave informed consent in accordance with the University of California at San Diego and San Diego State University Institutional Review Boards.

MRI Acquisition

Imaging data were acquired on a GE 3 Tesla MR750 scanner with an eight-channel head coil. High-resolution structural images were acquired with a standard fast spoiled gradient-recalled echo T1-weighted sequence (repetition time [TR], 11.08 ms; echo time [TE], 4.3 ms; flip angle, 45°; field of view, 256 mm; matrix, 256 × 256; 180 slices; 1 mm^3 resolution). Functional T2-weighted images were obtained using a single-shot, gradient-recalled,

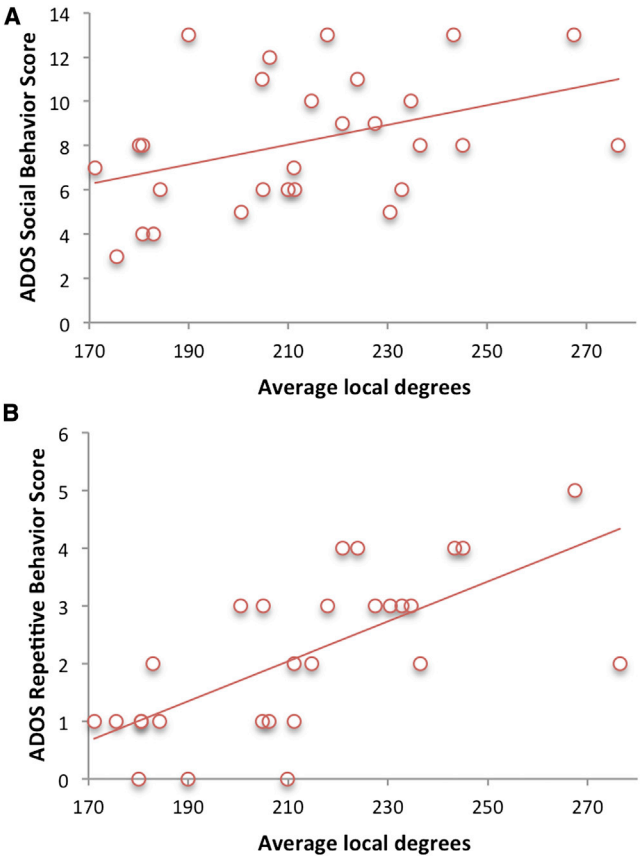

Figure 2. Correlations between Local Connection Density and Symptom Severity

(A and B) Correlations of average local degrees in clusters of significant group differences (all clusters in Figures 1D and 1E combined) with ADOS social (A) and repetitive behavior scores (B) in the ASD group.

echo-planar pulse sequence. One 6:10 min resting-state scan was acquired consisting of 185 whole-brain volumes (TR, 2,000 ms; TE, 30 ms; slice thickness, 3.4 mm; flip angle, 90°; field of view, 220 mm; matrix, 64 × 64). The first five time points were discarded to allow for T1 equilibration effects, leaving 180 time points (6 min) for the analysis. Participants were instructed to relax and keep their eyes directed on a cross-hair in the center of a back-projection screen for the duration of the scan.

Data Preprocessing

Data were processed using the Analysis of Functional NeuroImages software (Cox, 1996; http://afni.nimh.nih.gov) and FSL 5.0 (Smith et al., 2004; http://www.fmrib.ox.ac.uk/fsl). Functional images were slice-time corrected, motion corrected (3dvolreg) to align to the middle time point, field-map corrected, and aligned to the anatomical image using FLIRT (Jenkinson et al., 2002; Jenkinson and Smith, 2001) with six degrees of freedom. FSL's nonlinear registration tool (FNIRT) was used to standardize images to the MNI152 standard image (3 mm isotropic) using sinc interpolation, and the outputs were blurred to a global full-width-at-half-maximum of 6 mm. Given recent concerns that traditional filtering approaches can cause rippling of motion confounds to neighboring time points (Carp, 2013), we used a second-order band-pass Butterworth filter (Power et al., 2013; Satterthwaite et al., 2013) to isolate low-frequency BOLD fluctuations ($0.008 < f < 0.08$ Hz; Cordes et al., 2001).

Regression of a total of 16 nuisance variables was performed to improve data quality (Satterthwaite et al., 2013). Nuisance regressors included six rigid-body motion parameters derived from motion correction and their derivatives. White matter and ventricular masks were created at the participant level using FSL's FAST image segmentation (Zhang et al., 2001) and trimmed to avoid partial-volume effects. An average time series was extracted from each mask and was removed using regression, along with its corresponding derivative. All nuisance regressors were band-pass filtered using the second-order Butterworth filter ($0.008 < f < 0.08$ Hz; Power et al., 2012; Satterthwaite et al., 2013). Global signal regression (GSR) was not performed in our primary analyses to avoid the creation of spurious anticorrelations (Murphy et al., 2009), which may confound between-group comparisons (Jones et al., 2010; Saad et al., 2012). However, additional analyses including GSR were performed and results are presented in the supplement (Figure S1).

Motion

Motion was quantified as the Euclidean distance between the six rigid-body motion parameters for two consecutive time points. For any instance >1.0 mm, considered excessive motion, the time point as well as the preceding and following time points were censored, or "scrubbed" (Power et al., 2012). If two censored time points occurred within ten time points of each other, all time points between them were also censored. In six ASD participants, fewer than 80% of time points remained after censoring. These participants were excluded from further analysis. In the final sample of 58 participants, only a total of 84 time points across nine TD participants and a total of 80 time points across seven ASD participants had to be censored. Average head motion over each participant's session was defined as the root mean square of displacement and did not significantly differ between groups ($p = 0.78$). For more detailed analysis of head motion, a two-way ANOVA was also conducted to test the effects of group and type of motion (three translational and three rotational). The interaction of between-group and motion type was not significant, $F(5,342) = 0.307$, $p = 0.91$. The interaction of between-group and motion type was also not significant when low- and higher-severity ASD subgroups (see below) were compared to the TD group, $F(5,162) = 0.112$, $p = 0.99$. This indicates that group differences shown in Figures 1C–1E were unlikely to be driven by motion or type of motion. However, for further protection and based on findings of regionally specific effects of motion (Satterthwaite et al., 2013; Yan et al., 2013), we performed a voxelwise whole-brain analysis testing for correlations between head motion (mean root square of displacement) and local density. Findings are presented in Figure S2A. An additional conjunction view presented in Figure S2B shows that areas of strong correlation between motion and local density only showed minimal overlap with clusters of between-group effects. Finally, we performed an analysis for a low-motion subsample, including 22 TD and 20 ASD participants matched for age ($p = 0.65$), nonverbal IQ ($p = 0.77$), and motion ($p = 0.84$), using a more conservative head motion threshold of >0.25 mm for censoring (Figure S2C).

Connectivity Density

Following an approach previously used in neurotypical adults by Sepulcre et al. (2010), we examined local and long-distance functional connectivity for each voxel. Voxels with $r > 0.25$ ($p < 0.001$) were considered functionally connected, applying a threshold used in previous studies (Buckner et al., 2009; Sepulcre et al., 2010). A secondary analysis using a more conservative threshold ($r > 0.50$) was also performed, and results are presented in the supplement (Figure S3). Using metrics from graph theory, the measure of *local degrees* was defined for each voxel as the number of connected neighboring voxels within a 14 mm radius to the reference voxel, using the Euclidean distance between the centers of voxel pairs. To generate a connectivity map for each group and degree metric, we converted local degrees to *Z* scores scores for each individual participant. For within-group maps, these *Z* scores scores were averaged across participants from each group. For group comparisons, *Z* scores were entered into voxelwise two-sample Student's t tests. To correct for multiple comparisons, we used Monte Carlo simulations (Forman et al., 1995) via AFNI's 3dclustsim command (uncorrected threshold: $p < 0.05$; minimum cluster volume: 50 voxels; corrected threshold: $p < 0.05$).

We further examined the relationship between local connectivity and symptom severity, focusing on regions with significant group differences. Clusters of overconnectivity (all yellow clusters in Figure 1C) and clusters of underconnectivity (all blue clusters in Figure 1C) were combined, respectively, and

Pearson's correlation analyses were performed between the mean number of local connections for each and three ADOS scores (as listed in Table 1).

Secondary Analyses for ASD Severity Subgroups

To assess in greater depth how the severity of symptoms impacted the regional patterns of local functional connectivity, we divided the ASD group into low- and higher-severity groups of equal size. We used a custom-made in-house script to examine all possible partitions, retaining those tightly matched on motion ($p > 0.9$) and moderately matched on age and nonverbal IQ ($p > 0.4$). Of the remaining partitions, the script then selected the one that maximized the differences in ADOS scores (Table S2).

SUPPLEMENTAL INFORMATION

Supplemental Information includes three figures and four tables and can be found with this article online at http://dx.doi.org/10.1016/j.celrep.2013.10.003.

ACKNOWLEDGMENTS

This study was supported by the National Institutes of Health (R01-MH081023) with additional funding from Autism Speaks (Dennis Weatherstone Predoctoral Fellowship 7850 to A.N.) and NIH T32-MH020068 (to P.S.). Special thanks to the participants and their families.

Received: January 18, 2013
Revised: September 3, 2013
Accepted: October 1, 2013
Published: November 7, 2013

REFERENCES

Amaral, D.G., Schumann, C.M., and Nordahl, C.W. (2008). Neuroanatomy of autism. Trends Neurosci. *31*, 137–145.

American Psychiatric Association. (2000). Diagnostic and Statistical Manual of Mental Disorders - IV - TR, Fourth Edition (Washington, DC: American Psychiatric Association).

Belmonte, M.K., Allen, G., Beckel-Mitchener, A., Boulanger, L.M., Carper, R.A., and Webb, S.J. (2004a). Autism and abnormal development of brain connectivity. J. Neurosci. *24*, 9228–9231.

Belmonte, M.K., Cook, E.H., Jr., Anderson, G.M., Rubenstein, J.L., Greenough, W.T., Beckel-Mitchener, A., Courchesne, E., Boulanger, L.M., Powell, S.B., Levitt, P.R., et al. (2004b). Autism as a disorder of neural information processing: directions for research and targets for therapy. Mol. Psychiatry *9*, 646–663.

Buckner, R.L., Sepulcre, J., Talukdar, T., Krienen, F.M., Liu, H., Hedden, T., Andrews-Hanna, J.R., Sperling, R.A., and Johnson, K.A. (2009). Cortical hubs revealed by intrinsic functional connectivity: mapping, assessment of stability, and relation to Alzheimer's disease. J. Neurosci. *29*, 1860–1873.

Carp, J. (2013). Optimizing the order of operations for movement scrubbing: Comment on Power et al. Neuroimage *76*, 436–438.

Casanova, M., and Trippe, J. (2009). Radial cytoarchitecture and patterns of cortical connectivity in autism. Philos. Trans. R. Soc. Lond. B Biol. Sci. *364*, 1433–1436.

CDC. (2012). Prevalence of autism spectrum disorders–Autism and Developmental Disabilities Monitoring Network, 14 sites, United States, 2008. MMWR Surveill. Summ. *61*, 1–19.

Cordes, D., Haughton, V.M., Arfanakis, K., Carew, J.D., Turski, P.A., Moritz, C.H., Quigley, M.A., and Meyerand, M.E. (2001). Frequencies contributing to functional connectivity in the cerebral cortex in "resting-state" data. AJNR Am. J. Neuroradiol. *22*, 1326–1333.

Courchesne, E., Campbell, K., and Solso, S. (2011a). Brain growth across the life span in autism: age-specific changes in anatomical pathology. Brain Res. *1380*, 138–145.

Courchesne, E., Mouton, P.R., Calhoun, M.E., Semendeferi, K., Ahrens-Barbeau, C., Hallet, M.J., Barnes, C.C., and Pierce, K. (2011b). Neuron number and size in prefrontal cortex of children with autism. JAMA *306*, 2001–2010.

Cox, R.W. (1996). AFNI: software for analysis and visualization of functional magnetic resonance neuroimages. Comput. Biomed. Res. *29*, 162–173.

Dakin, S., and Frith, U. (2005). Vagaries of visual perception in autism. Neuron *48*, 497–507.

Forman, S.D., Cohen, J.D., Fitzgerald, M., Eddy, W.F., Mintun, M.A., and Noll, D.C. (1995). Improved assessment of significant activation in functional magnetic resonance imaging (fMRI): use of a cluster-size threshold. Magn. Reson. Med. *33*, 636–647.

Geschwind, D.H., and Levitt, P. (2007). Autism spectrum disorders: developmental disconnection syndromes. Curr. Opin. Neurobiol. *17*, 103–111.

Happé, F. (1999). Autism: cognitive deficit or cognitive style? Trends Cogn. Sci. *3*, 216–222.

Hill, E.L. (2004). Executive dysfunction in autism. Trends Cogn. Sci. *8*, 26–32.

Jenkinson, M., and Smith, S. (2001). A global optimisation method for robust affine registration of brain images. Med. Image Anal. *5*, 143–156.

Jenkinson, M., Bannister, P., Brady, M., and Smith, S. (2002). Improved optimization for the robust and accurate linear registration and motion correction of brain images. Neuroimage *17*, 825–841.

Jones, T.B., Bandettini, P.A., Kenworthy, L., Case, L.K., Milleville, S.C., Martin, A., and Birn, R.M. (2010). Sources of group differences in functional connectivity: an investigation applied to autism spectrum disorder. Neuroimage *49*, 401–414.

Kim, Y.S., Leventhal, B.L., Koh, Y.J., Fombonne, E., Laska, E., Lim, E.C., Cheon, K.A., Kim, S.J., Kim, Y.K., Lee, H., et al. (2011). Prevalence of autism spectrum disorders in a total population sample. Am. J. Psychiatry *168*, 904–912.

Lord, C., Rutter, M., DiLavore, P., and Risi, S. (2001). Autism Diagnostic Observation Schedule (Los Angeles: Western Psychological Services).

Mottron, L., Dawson, M., Soulières, I., Hubert, B., and Burack, J. (2006). Enhanced perceptual functioning in autism: an update, and eight principles of autistic perception. J. Autism Dev. Disord. *36*, 27–43.

Murphy, K., Birn, R.M., Handwerker, D.A., Jones, T.B., and Bandettini, P.A. (2009). The impact of global signal regression on resting state correlations: are anti-correlated networks introduced? Neuroimage *44*, 893–905.

Oldfield, R.C. (1971). The assessment and analysis of handedness: the Edinburgh inventory. Neuropsychologia *9*, 97–113.

Power, J.D., Barnes, K.A., Snyder, A.Z., Schlaggar, B.L., and Petersen, S.E. (2012). Spurious but systematic correlations in functional connectivity MRI networks arise from subject motion. Neuroimage *59*, 2142–2154.

Power, J.D., Barnes, K.A., Snyder, A.Z., Schlaggar, B.L., and Petersen, S.E. (2013). Steps toward optimizing motion artifact removal in functional connectivity MRI; a reply to Carp. Neuroimage *76*, 439–441.

Rippon, G., Brock, J., Brown, C., and Boucher, J. (2007). Disordered connectivity in the autistic brain: challenges for the "new psychophysiology". Int. J. Psychophysiol. *63*, 164–172.

Rubenstein, J.L., and Merzenich, M.M. (2003). Model of autism: increased ratio of excitation/inhibition in key neural systems. Genes Brain Behav. *2*, 255–267.

Rutter, M., LeCouteur, A., and Lord, C. (2003). Autism Diagnostic Interview - R (Los Angeles: Wester Psychological Services).

Saad, Z.S., Gotts, S.J., Murphy, K., Chen, G., Jo, H.J., Martin, A., and Cox, R.W. (2012). Trouble at rest: how correlation patterns and group differences become distorted after global signal regression. Brain Connect. *2*, 25–32.

Samson, F., Mottron, L., Soulières, I., and Zeffiro, T.A. (2012). Enhanced visual functioning in autism: an ALE meta-analysis. Hum. Brain Mapp. *33*, 1553–1581.

Satterthwaite, T.D., Elliott, M.A., Gerraty, R.T., Ruparel, K., Loughead, J., Calkins, M.E., Eickhoff, S.B., Hakonarson, H., Gur, R.C., Gur, R.E., and Wolf, D.H. (2013). An improved framework for confound regression and filtering for

control of motion artifact in the preprocessing of resting-state functional connectivity data. Neuroimage *64*, 240–256.

Sepulcre, J., Liu, H., Talukdar, T., Martincorena, I., Yeo, B.T., and Buckner, R.L. (2010). The organization of local and distant functional connectivity in the human brain. PLoS Comput. Biol. *6*, e1000808.

Shen, M.D., Shih, P., Öttl, B., Keehn, B., Leyden, K.M., Gaffrey, M.S., and Müller, R.A. (2012). Atypical lexicosemantic function of extrastriate cortex in autism spectrum disorder: evidence from functional and effective connectivity. Neuroimage *62*, 1780–1791.

Shukla, D.K., Keehn, B., and Müller, R.-A. (2011). Tract-specific analyses of diffusion tensor imaging show widespread white matter compromise in autism spectrum disorder. J. Child Psychol. Psychiatry *52*, 286–295.

Simmons, D.R., Robertson, A.E., McKay, L.S., Toal, E., McAleer, P., and Pollick, F.E. (2009). Vision in autism spectrum disorders. Vision Res. *49*, 2705–2739.

Smith, S.M., Jenkinson, M., Woolrich, M.W., Beckmann, C.F., Behrens, T.E., Johansen-Berg, H., Bannister, P.R., De Luca, M., Drobnjak, I., Flitney, D.E., et al. (2004). Advances in functional and structural MR image analysis and implementation as FSL. Neuroimage *23* (*Suppl 1*), S208–S219.

State, M.W., and Šestan, N. (2012). Neuroscience. The emerging biology of autism spectrum disorders. Science *337*, 1301–1303.

Tyszka, J.M., Kennedy, D.P., Paul, L.K., and Adolphs, R. (2013). Largely typical patterns of resting-state functional connectivity in high-functioning adults with autism. Cereb. Cortex. Published online February 20, 2013. http://dx.doi.org/10.1093/cercor/bht040.

Van Dijk, K.R., Hedden, T., Venkataraman, A., Evans, K.C., Lazar, S.W., and Buckner, R.L. (2010). Intrinsic functional connectivity as a tool for human connectomics: theory, properties, and optimization. J. Neurophysiol. *103*, 297–321.

Van Dijk, K.R., Sabuncu, M.R., and Buckner, R.L. (2012). The influence of head motion on intrinsic functional connectivity MRI. Neuroimage *59*, 431–438.

Vissers, M.E., Cohen, M.X., and Geurts, H.M. (2012). Brain connectivity and high functioning autism: a promising path of research that needs refined models, methodological convergence, and stronger behavioral links. Neurosci. Biobehav. Rev. *36*, 604–625.

Wechsler, D. (1999). Wechsler Abbreviated Scale of Intelligence (WASI) (San Antonio: Psychological Corporation).

Wolff, J.J., Gu, H., Gerig, G., Elison, J.T., Styner, M., Gouttard, S., Botteron, K.N., Dager, S.R., Dawson, G., Estes, A.M., et al. (2012). Differences in white matter fiber tract development present from 6 to 24 months in infants with autism. Am. J. Psychiatry *169*, 589–600.

Yan, C.G., Cheung, B., Kelly, C., Colcombe, S., Craddock, R.C., Di Martino, A., Li, Q., Zuo, X.N., Castellanos, F.X., and Milham, M.P. (2013). A comprehensive assessment of regional variation in the impact of head micromovements on functional connectomics. Neuroimage *76*, 183–201.

Zhang, Y., Brady, M., and Smith, S. (2001). Segmentation of brain MR images through a hidden Markov random field model and the expectation-maximization algorithm. IEEE Trans. Med. Imaging *20*, 45–57.